

This discussion paper is/has been under review for the journal Atmospheric Chemistry and Physics (ACP). Please refer to the corresponding final paper in ACP if available.

Insights into hydroxyl measurements and atmospheric oxidation in a California forest

J. Mao^{1,*}, X. Ren^{1,}, W. H. Brune¹, D. M. Van Duin¹, R. C. Cohen², J.-H. Park³, A. H. Goldstein³, F. Paulot⁴, M. R. Beaver⁴, J. D. Crouse⁴, P. O. Wennberg⁴, J. P. DiGangi^{5,***}, S. B. Henry⁵, F. N. Keutsch⁵, C. Park^{6,****}, G. W. Schade⁶, G. M. Wolfe^{7,*****}, and J. A. Thornton⁷**

¹Department of Meteorology, Pennsylvania State University, University Park, PA, USA

²Department of Chemistry and Department of Earth and Planetary Science, University of California Berkeley, Berkeley, CA, USA

³Department of Environmental Science, Policy, and Management, University of California Berkeley, Berkeley, CA, USA

⁴Division of Geological and Planetary Sciences, California Institute of Technology, Pasadena, CA, USA

⁵Department of Chemistry, University of Wisconsin-Madison, Madison, Wisconsin, USA

⁶Department of Atmospheric Sciences, Texas A&M University, College Station, TX, USA

⁷Department of Atmospheric Sciences, University of Washington, Seattle, WA, USA

Insights into hydroxyl measurements in a forest

J. Mao et al.

Title Page

Abstract

Introduction

Conclusions

References

Tables

Figures

◀

▶

◀

▶

Back

Close

Full Screen / Esc

Printer-friendly Version

Interactive Discussion



* now at: Geophysical Fluid Dynamics Laboratory, NOAA, Princeton, NJ, USA

** now at: Air Resources Laboratory, NOAA, Silver Spring, MD, USA

*** now at: Department of Civil and Environmental Engineering, Princeton University, Princeton, NJ, USA

**** now at: Department of Atmospheric and Oceanic Sciences, University of California, Los Angeles, CA, USA

***** now at: Department of Chemistry, University of Wisconsin-Madison, Madison, Wisconsin, USA

Received: 22 February 2012 – Accepted: 23 February 2012 – Published: 2 March 2012

Correspondence to: J. Mao (jingqiu.mao@noaa.gov)

Published by Copernicus Publications on behalf of the European Geosciences Union.

ACPD

12, 6715–6744, 2012

Insights into hydroxyl measurements in a forest

J. Mao et al.

Title Page

Abstract

Introduction

Conclusions

References

Tables

Figures

⏪

⏩

◀

▶

Back

Close

Full Screen / Esc

Printer-friendly Version

Interactive Discussion



Abstract

The understanding of oxidation in forest atmospheres is being challenged by measurements of unexpectedly large amounts of hydroxyl (OH). A significant number of these OH measurements were made by laser-induced fluorescence in low-pressure detection chambers (called Fluorescence Assay with Gas Expansion (FAGE)) using the Penn State Ground-based Tropospheric Hydrogen Oxides Sensor (GTHOS). We deployed a new chemical removal method to measure OH in parallel with the traditional FAGE method. The new method gives on average only 40–50 % of the OH from the traditional method and this discrepancy is temperature-dependent. Evidence indicates that the new method measures atmospheric OH while the traditional method is affected by internally generated OH, possibly from oxidation of biogenic volatile organic compounds. The agreement between OH measured by this new technique and modeled OH suggests that oxidation chemistry in at least one forest atmosphere is better understood than previously thought.

1 Introduction

Forests emit copious amounts of biogenic volatile organic compounds (BVOCs) that react with ozone (O_3) and the hydroxyl radical (OH), thus creating many more oxidized volatile and semi-volatile chemicals. In the absence of nitric oxide (NO), a condition typical for remote forests, the oxidation chemistry removes ozone, regenerates some OH, removes hydrogen oxides by reactions among hydroperoxyl (HO_2) and organoperoxy (RO_2) radicals, and produces semi-volatile secondary organic aerosols (SOA). The extensive global coverage of remote forests (Hansen et al., 2003) means that atmospheric chemistry of remote forests influences global oxidation capacity, ozone budget, SOA distribution, and the atmospheric lifetime of methane.

OH plays a central role in these atmosphere-biosphere interactions because OH oxidizes most of the BVOCs emitted in remote forests. However, several field studies in

Insights into hydroxyl measurements in a forest

J. Mao et al.

Title Page

Abstract

Introduction

Conclusions

References

Tables

Figures



Back

Close

Full Screen / Esc

Printer-friendly Version

Interactive Discussion



Insights into hydroxyl measurements in a forestJ. Mao et al.

[Title Page](#)[Abstract](#)[Introduction](#)[Conclusions](#)[References](#)[Tables](#)[Figures](#)[⏪](#)[⏩](#)[◀](#)[▶](#)[Back](#)[Close](#)[Full Screen / Esc](#)[Printer-friendly Version](#)[Interactive Discussion](#)

terrestrial vegetation have shown that measured OH exceeds modeled OH by a factor of 2 to 10 (Tan et al., 2001; Thornton et al., 2002; Lelieveld et al., 2008; Ren et al., 2008; Hofzumahaus et al., 2009; Whalley et al., 2011), thus indicating the chemistry of BVOCs is poorly understood. This discrepancy presents a challenge: the OH production rate needed to maintain these measured OH abundances is 2–10 times larger than current model mechanisms can support and would produce large amounts of HO₂ and RO₂ radicals (Faloona et al., 2001; Tan et al., 2001). However, such high levels of HO₂ and RO₂ were not observed (Ren et al., 2008; Hofzumahaus et al., 2009; Whalley et al., 2011). These OH discrepancies helped motivate the development of new improved isoprene oxidation mechanisms, but they generally have not been able to explain the OH measurements (Butler et al., 2008; Hofzumahaus et al., 2009; Paulot et al., 2009a,b; Peeters et al., 2009; Peeters and Müller, 2010).

An alternate explanation is that our OH measurements are wrong. The majority of all OH measurements in and above remote forests have been made with laser induced fluorescence in low-pressure detection cells (often called Fluorescence Assay with Gas Expansion (FAGE)) (Hard et al., 1984), and several of them by the Penn State instrument, the Ground-based Tropospheric Hydrogen Oxides Sensor (GTHOS). In this method, air is sampled through a pinhole. The OH absorbs light from a tunable, pulsed UV laser and then its fluorescence is detected tens of nanoseconds later with a gated detector. The OH fluorescence signal is separated from the background signal by periodically shifting the laser wavelength from an OH absorption line to nearby off-line wavelengths. OH generated by the laser and several other interferences have been ruled out by laboratory and field studies for GTHOS (Ren et al., 2004) and the fluorescence spectrum of the signal matches that of OH. However, it is possible that BVOC oxidation products rapidly form OH after entering the instrument inlet and that this conversion is responsible for the inexplicably high OH measurements in prior studies.

To test this possibility, we added a second method for detecting OH for a multi-investigator field campaign in a Sierra Nevada forest during summer 2009. In the

second method, a chemical that removes OH was periodically added to the air just before it was sampled by the instrument. This zeroing method has been used previously by Chemical Ionization Mass Spectrometer instruments (Tanner et al., 1997) with the chemical being either propane or hexafluoropropene (C₃F₆). We primarily used C₃F₆ because of its chemical and optical properties (Dubey et al., 1996), but also used propane during one day of the study. Here, we discuss the comparison of these two simultaneous OH measurements with each other and with a photochemical box model that has recent updates in BVOC oxidation mechanisms. Simultaneous measurements of the OH reactivity and of the hydroperoxyl radical (HO₂) provide additional information about the comparisons.

2 Methodology

2.1 Site description

The Biosphere Effects on Aerosols and Photochemistry Experiment II (BEARPEX09, <http://www.ocf.berkeley.edu/~bearpex/>) was aimed to examine the photochemistry in and above the forest canopy with a wide range of state-of-the-art measurement techniques. The field site is a Ponderosa pine plantation near the Blodgett Forest Research Station (BFRS) in the California Sierra Nevada Mountains. BFRS is located 75 km northeast of Sacramento, CA (1315 m a.s.l., 38.9° N, 120.6° W). The mean canopy height was 8.9 m. The site includes one 15 m walk-up tower in the south and one 18 m scaffolding tower in the north. Two towers were separated by 10 m. Most instruments were installed on the north tower, including meteorological sensors for temperature, pressure, relative humidity and wind speed. An electric boom lift, on which OH, HO₂ and OH reactivity instruments were installed, was adjacent to the north tower. A propane generator was located 125 m north of the north tower. The sampling site could be intermittently influenced by generator plumes at night (but not daytime). Typical meteorological conditions at the site are characterized by a dry season from May

Insights into hydroxyl measurements in a forest

J. Mao et al.

Title Page

Abstract

Introduction

Conclusions

References

Tables

Figures



Back

Close

Full Screen / Esc

Printer-friendly Version

Interactive Discussion



to September with high daytime temperature, low rainfall and low humidity, and consistent southwesterly (upslope) wind during the day and northeasterly (downslope) wind at night.

Local biogenic VOC emission at BFRS consists mainly of 2-methyl-3-buten-2-ol (MBO) (Schade et al., 2000), monoterpenes (particularly beta-pinene) (Bouvier-Brown et al., 2009a), sesquiterpenes (Bouvier-Brown et al., 2009b), and related oxygenated compounds (Holzinger et al., 2005). Recent studies also identified a number of previously unmeasured VOCs, such as sesquiterpenes, methyl chavicol (estragole), and related oxygenated compounds at BFRS (Bouvier-Brown et al., 2009c). Due to consistent southwesterly wind during daytime, BFRS is influenced by anthropogenic emissions from the Greater Sacramento Area (~ 75 km SW) and biogenic emissions from a 20–25 km wide band of oak woodlands (~ 30 km SW) during daytime (Dreyfus et al., 2002). The biogenic plume usually arrives at 12:00–14:00 Pacific Standard Time (PST) with relatively high levels of isoprene and its oxygenated products. The anthropogenic plume arrives at late afternoon between 18:00–20:00 PST with elevated levels of anthropogenic tracers (LaFranchi et al., 2009). Thus the mixture of biogenic and anthropogenic influences changes during the day.

2.2 Two methods of OH measurements

Observations of OH, HO₂ and OH reactivity were made from 20 June (day of year (DOY) = 171) to 30 July (DOY = 211) of 2009. OH and HO₂ were measured by the Penn State Ground-based Tropospheric Hydrogen Oxides Sensor (GTHOS) (Faloona et al., 2004) and OH reactivity was measured by the OH reactivity instrument from the same group (Mao et al., 2009). GTHOS and OH reactivity instrument were both installed on the lift. This lift was manually controlled to move from the ground to 17 m high (stopped at various heights) for the purpose of measuring vertical profile of radicals. Vertical profiling was conducted two to three times per day. For the rest of the time, the lift was mainly kept at a height of 9, 12, or 15 m. As little variability was found for OH, HO₂ and OH reactivity at these three heights (less than 20 %), we here use the measurements

Insights into hydroxyl measurements in a forest

J. Mao et al.

Title Page

Abstract

Introduction

Conclusions

References

Tables

Figures

◀

▶

◀

▶

Back

Close

Full Screen / Esc

Printer-friendly Version

Interactive Discussion



at all three heights to ensure sufficient data points.

OH was measured by Laser Induced Fluorescence (LIF) technique in a low pressure chamber (Faloona et al., 2004). OH absorbs laser light at a wavelength near 308 nm and the excited OH emits fluorescence in the wavelength range from 307 to 311 nm simultaneously. The fluorescence photons are captured by a gated microchannel plate (MCP) detector, which is set perpendicular to the airflow and the laser beam. HO₂ is converted to OH via its reaction with NO followed by the LIF measurement in a second detection axis of the GTHOS system. The laser system consists of a dye laser that is pumped by a diode-pumped Nd:YAG laser (Spectra-Physics, X30SC-1060A) at 3 kHz pulse repetition. The output of the dye laser is used to excite OH. Tuning of the laser wavelength is achieved by an etalon. The etalon is tuned so that the laser wavelength remains on-line of an OH absorption line for 10 s and then nearby off-line wavelengths for 10 s to measure the background. The difference in the average on-line and average off-line signals is the OH fluorescence signal, which is converted to an OH mixing ratio by calibrations with a known amount of OH. The measured OH in this approach is called "OHwave".

The second approach to measure OH is chemical modulation using the signal difference with and without the addition of high-purity gaseous perfluoropropene (C₃F₆) to remove OH prior to the detection by LIF (Fig. 1). C₃F₆ is ideal as an OH scrubber as it reacts fast enough to remove OH in milliseconds without propagating radicals or complicating secondary chemistry. Its optical absorption around 308 nm is also negligible (Dubey et al., 1996). In order to inject C₃F₆ into the upstream of inlet flow, a 4 cm-long aluminum cylinder (OD 5.1 cm and ID 2.5 cm) was installed on top of the GTHOS inlet. A 5-cm long PFA tube with ID of 1.2 cm was installed inside this cylinder to reduce the residence time of ambient air inside the cylinder. This setup also minimized the wall loss of OH and HO₂ radicals prior to entering the GTHOS inlet. Gaseous C₃F₆ was injected simultaneously through four 0.25 mm needles pointed toward the center, which were located about 4 cm above the inlet (Fig. 2). C₃F₆ was added for two minutes every four minutes at a flow rate of 5 standard cubic centimeters per minute (sccm). An N₂

Insights into hydroxyl measurements in a forest

J. Mao et al.

Title Page

Abstract

Introduction

Conclusions

References

Tables

Figures

◀

▶

◀

▶

Back

Close

Full Screen / Esc

Printer-friendly Version

Interactive Discussion



flow of 100 sccm was continuously added through the needles so that the periodic C_3F_6 addition did not perturb the flow. This injection system, without C_3F_6 addition, caused negligible OH loss according to tests in which the injection system was occasionally removed for an hour and the OHwave signal did not change. On one day, propane was substituted for C_3F_6 with similar results. The difference in signal with and without the addition of C_3F_6 is used to calculate the measured OH that is defined as "OHchem".

In some instrument configurations, OH can be generated by the 308 nm laser beam inside the instrument. This laser-generated OH has been observed in some LIF systems, including a previous version of GTHOS, from the photolysis of ozone followed by the reaction of excited state oxygen atoms with H_2O (Smith and Crosley, 1990). The generation of OH by the laser can be tested by varying the laser power because laser-generated OH requires two photons – one to make OH and one to detect it – so that the amount of detected laser-generated OH depends on the square of the laser power. The current version of GTHOS was designed and tested to minimize laser-generated OH. Also, a filter wheel has been used to suddenly attenuate the laser power to the OH detection axis so that the laser power dependence of the OH signal can always be tested.

2.3 Model simulation

A photochemical box model is used to examine the OH and HO_2 measurements during BEARPEX09. The model uses the Regional Atmospheric Chemistry Mechanism, Version 2 (RACM2) (Henderson et al., 2011), modified with isoprene nitrate chemistry (Paulot et al., 2009a) and isoprene epoxide chemistry (Paulot et al., 2009b), reduced unimolecular isomerization of isoprene hydroxyperoxy radicals (Peeters et al., 2009; Peeters and Müller, 2010; Crouse et al., 2011), terpene oxidation (Wolfe and Thornton, 2011), and MBO oxidation (Carrasco et al., 2007; Steiner et al., 2007; Chan et al., 2009). Photolysis rates were calculated by the Tropospheric Ultraviolet and Visible (TUV) radiation model (<http://www.acd.ucar.edu/TUV>) and then scaled based on the local Photosynthetically Active Radiation (PAR) measurements. The model was

Insights into hydroxyl measurements in a forest

J. Mao et al.

Title Page

Abstract

Introduction

Conclusions

References

Tables

Figures

◀

▶

◀

▶

Back

Close

Full Screen / Esc

Printer-friendly Version

Interactive Discussion



constrained by measured meteorological parameters and chemical species (Table S1) and run one day for each data point, long enough to allow most calculated species to reach steady state but short enough to prevent the buildup of secondary products. Dry deposition was assumed for aldehydes and peroxides with a lifetime of 30 h (Karl et al., 2010). This box model is similar to other commonly used box models. The model simulation used in the main body represents the best knowledge of our current understanding of biogenic oxidation chemistry. Meanwhile, we have conducted model simulations with a variety of chemical mechanisms, which can be found in the supplement material.

Following Fuchs et al. (2011), we conducted RO_2 interference tests in the laboratory with the same configuration deployed in the field for isoprene and several alkenes. The relative detection sensitivities are roughly 0.6. Therefore we corrected HO_2 measurements based on modeled isoprene peroxy radical (ISOP), peroxy radicals from MACR (MACRO2 and MAO3) and peroxy radical from MVK (MVKO2) with a relative sensitivity of 0.6. RO_2 from MBO are not included, as measurements from MBO hydroperoxide indicates a much lower level of MBO peroxy radical than model calculations, likely due to unknown removal mechanism of MBO RO_2 .

3 Results

3.1 Diurnal cycle

Figure 1 shows the diurnal cycle of measured and modeled OH between 20 June and 30 July 2009 near the Blodgett Forest Research Station (BFRS). While OH_{wave} and OH_{chem} show a similar diurnal pattern, OH_{chem} is only 40% of OH_{wave} during daytime and 50% at night, on average. The question is then “Which one is the real OH?”

We first quantify the extent to which external OH is removed with the external C_3F_6 addition. A mercury lamp with 185 nm UV light emission was placed on the outer wall of

Insights into hydroxyl measurements in a forest

J. Mao et al.

Title Page

Abstract

Introduction

Conclusions

References

Tables

Figures

◀

▶

◀

▶

Back

Close

Full Screen / Esc

Printer-friendly Version

Interactive Discussion



the aluminum cylinder (Hg lamp 1 in Fig. 2). This lamp was turned on for 10 min every 4 h to produce OH by photolyzing ambient water vapor: $\text{H}_2\text{O} + h\nu \rightarrow \text{OH} + \text{H}$, where H immediately combines with O_2 to form HO_2 . This externally generated OH signal was two orders of magnitude larger than ambient OH and C_3F_6 addition removed $94 \pm 5\%$ of this signal (Fig. 3). The near-complete removal of OH generated is the primary evidence that OHchem is the real OH and that OHwave is influenced by OH generated within GTHOS.

We then quantify the uncertainty due to the internal OH removal with the external C_3F_6 addition, by generating OH in two locations above the OH detection axis during laboratory studies. One lamp was placed just below the inlet (Hg lamp 2 in Fig. 2), generating OH in the sampled flow and a second lamp was added just above the detection axis (Hg lamp 3 in Fig. 2) and generated OH in the detection axis itself. Both lamps were shrouded so that their light shone only across the flow tube and not up into the inlet or down into the detection cell. We find that C_3F_6 addition removed none of the OH generated in the OH detection axis but 60 % of the OH generated just below the instrument pinhole inlet. Because it is not known for certain that the OH is generated near the inlet, we assume 30 % (average between 0 and 60 %) for this removal and increase the measurement uncertainty accordingly. In any case, this evidence demonstrates that OHchem is within 30 % of the real OH, depending on where the internal OH is generated.

Three lines of evidence indicate that the signals observed in BEARPEX09 were not laser generated. First, the observed OH signal was proportional to the laser power, not quadratic. Second, the large difference for OH removal for the internal OH generation between near the inlet and near the detection axis indicates that the difference between OHwave and OHchem is not generated by the UV laser in the detection axis. Third, a recent laboratory test for α -pinene under high ozone showed no laser power dependence of the OH signal with C_3F_6 on or off. Thus, any differences observed between OHwave and OHchem are not due to laser-generated OH.

OHchem is in much better agreement with modeled OH than is OHwave (Fig. 3).

Insights into hydroxyl measurements in a forest

J. Mao et al.

Title Page

Abstract

Introduction

Conclusions

References

Tables

Figures

◀

▶

◀

▶

Back

Close

Full Screen / Esc

Printer-friendly Version

Interactive Discussion



The difference between OHwave and the model is statistically significant while the difference between OHchem and the model is not. Considering the partial chemical removal of internally generated OH by C₃F₆ addition, the agreement between OHchem and modeled OH is well within the combined uncertainties. Thus the modeled OH is consistent with the real OH.

Nighttime OHchem also agrees better with modeled OH. A discrepancy between measured and modeled OH at night has been widely observed with the Penn State Ground-based Tropospheric Hydrogen Oxides Sensor (GTHOS) for OHwave, for which the measurement is typically 3 to 10 times the modeled nighttime OH (Faloona et al., 2001). Since OHchem ($3.4 \pm 1.4 \times 10^5$ molecules cm⁻³) is about half of OHwave ($7.5 \pm 0.8 \times 10^5$ molecules cm⁻³) during night (22:00 to 04:00 PST), the discrepancy between measured and modeled OH ($2.4 \pm 0.6 \times 10^5$ molecules cm⁻³) is largely improved.

Figure 4 shows the diurnal cycle of measured and modeled HO₂ and OH reactivity between 20 June and 30 July 2009 near BFRS. In general both measured HO₂ and OH reactivity are in good agreement with modeled values, although some large overestimates of HO₂ were found for the model using the fast isomerization rates calculated by Peeters et al. (Peeters et al., 2009; Peeters and Müller, 2010) (Fig. S2). The difference between measured OH reactivity and the calculated OH reactivity from available measurements can be significantly improved by the inclusion of oxidation products from the model. We will further discuss these model-to-observation comparisons of HO₂ and OH reactivity in the next section.

3.2 Temperature dependence

Another remarkable feature is the observed temperature dependence for the discrepancy between OHwave and OHchem (Fig. 5a). OHwave agrees with OHchem for temperatures near 295 K but becomes more than twice as large above 300 K. The modeled OH has a smaller temperature dependence similar to that of OHchem. Interestingly, the difference between OHwave and OHchem correlates with the OH reactivity ($r^2 = 0.94$

Insights into hydroxyl measurements in a forest

J. Mao et al.

Title Page

Abstract

Introduction

Conclusions

References

Tables

Figures

◀

▶

◀

▶

Back

Close

Full Screen / Esc

Printer-friendly Version

Interactive Discussion



for median values in Fig. 6), suggesting that laboratory studies should focus on BVOCs or their oxidation products in a search to explain this interference. A question is “What causes this interference signal?”

The spectrum of the interference signal matched the OH spectrum, implying that some chemical enters the GTHOS and then rapidly produces OH. After passing through the inlet hole, the sampled air experiences a supersonic isentropic gas expansion due to the sharp pressure change from one atmosphere to ~ 5 hPa and cools by more than 150 K (Stevens et al., 1994; Heal et al., 1995). The air then goes through a Mach disc and warms rapidly to approximately ambient temperature before it reaches the detection axis (Stevens et al., 1994; Heal et al., 1995). Such strong gradients of temperature and pressure could favor the dissociation of certain intermediate species.

Laboratory evidence indicates that some intermediate species from ozonolysis (Kurpius and Goldstein, 2003; Fares et al., 2010) tend to promptly decompose and produce OH at low pressure (Kroll et al., 2001; Donahue et al., 2011). Examples are the Criegee Intermediates and vinyl hydroperoxide (Herrmann et al., 2010), which promptly decompose on a short time scale ($< 10 \mu\text{s}$) (Zhang et al., 2002). It is also possible that such intermediate species come from other pathways. For instance, C5-hydroperoxyaldehydes (HPALDs), proposed by Peeters et al. (2009), appear to preferentially form at higher temperatures via peroxy radical isomerization for isoprene (Crouse et al., 2011).

Such behavior may not be limited to isoprene. In BEARPEX09, MBO is the dominant species for OH loss due its local emission and high reactivity with OH ($6.3 \times 10^{-11} \text{ molecules cm}^{-3} \text{ s}^{-1}$ at 300 K) (Baasandorj and Stevens, 2007). Despite the similar structure to isoprene, the model treatment of MBO photooxidation is completely different in terms of radical propagation. No OH-regenerating mechanism has been reported for the oxidation of MBO by OH (Carrasco et al., 2007; Chan et al., 2009). The mechanism proposed by Peeters et al. (Peeters et al., 2009; Peeters and Müller, 2010) is not applicable for MBO peroxy radicals as the H-shift isomerization (the main pathway for producing HPALDs and HO_x) requires that a 6- or 7-membered

Insights into hydroxyl measurements in a forest

J. Mao et al.

Title Page

Abstract

Introduction

Conclusions

References

Tables

Figures

◀

▶

◀

▶

Back

Close

Full Screen / Esc

Printer-friendly Version

Interactive Discussion



ring transition state can be formed between the peroxy radical and a labile hydrogen atom. Although no laboratory evidence currently supports any of these possibilities, a reasonable hypothesis is that the discrepancy between OHwave and OHchem is due to intermediate products from the oxidation of BVOCs.

5 Comparison of the measured and modeled HO₂ provides an additional constraint on the model (Fig. S3b). Using the fast isomerization rates calculated by Peeters et al. (Peeters et al., 2009; Peeters and Müller, 2010), the box model calculated HO₂ mixing ratios which are up to 3 times greater than the HO₂ measurements (Fig. S3), consistent with recent model-to-observation comparisons in other forest stud-
10 ies (Kanaya et al., 2011; Lu et al., 2011; Whalley et al., 2011). However, when the isomerization rate is reduced for the unimolecular isomerization channel in accordance with recent laboratory studies (Crouse et al., 2011), the HO₂ from the Peeters mechanism comes into better agreement with the HO₂ measurements (Fig. S3b). Slight overestimation of HO₂ could be attributed to an efficient aerosol reactive uptake (Mao et al., 2012), which is not included in the box model.

15 Comparison of the measured and calculated OH reactivity, the inverse of the OH lifetime, is another constraint. In a previous forest field campaign (PROPHET, 1998 and 2000), the measured OH reactivity was greater than the OH reactivity calculated using all available measurements (Di Carlo et al., 2004). This “missing OH reactivity”
20 had a temperature dependence that matched the temperature dependence commonly used for the emission of terpenes, which is $mOHR(T) = mOHR(293) \times \exp(0.11 \times (T - 293))$, where mOHR represents missing OH reactivity. During BEARPEX09, the measured OH reactivity also exceeded that of the calculated OH reactivity from individual measured species (Fig. 3c). The difference between the measured OH reactivity and that calculated using only measured species during BEARPEX09 is $mOHR(T) = mOHR(293) \times \exp(0.168 \times (T - 293))$. However, if the calculated OH reactivity includes reactions with modeled BVOC oxidation products (Table 1), then the measured and modeled OH reactivity agree well within the uncertainties (Fig. 5c).
25 Although MBO chemistry may not be well understood, the contribution of OH reactivity

Insights into hydroxyl measurements in a forest

J. Mao et al.

Title Page

Abstract

Introduction

Conclusions

References

Tables

Figures

◀

▶

◀

▶

Back

Close

Full Screen / Esc

Printer-friendly Version

Interactive Discussion



from modeled MBO oxidation products can still provide a useful and reasonable metric to constrain OH loss in the model. This agreement provides evidence that the missing OH reactivity is not mainly due to unmeasured BVOCs, such as unmeasured sesquiterpenes, but instead is due to oxidation products of measured BVOCs, consistent with recent investigations in the missing OH reactivity (Lou et al., 2010; Kim et al., 2011; Wolfe et al., 2011).

4 Discussion and conclusions

Several instrument comparisons for OH measurements have been conducted in the past two decades, to quantify the possible errors in our understanding of radical chemistry. The airborne comparisons suggest a relatively good agreement between two OH instruments. During the NASA PEM Tropics B aircraft campaign in 1999, OH was measured by both Penn State LIF instrument on the NASA DC-8 aircraft and NCAR CIMS instrument on the NASA P-3B aircraft. These side-by-side flight intercomparisons show a ratio of LIF/CIMS OH from 0.8 near surface to 1.6 at 8 km (Eisele et al., 2001). During the NASA TRACE-P aircraft campaign in 2001, the same two instruments show a ratio of LIF/CIMS OH roughly 0.7 for three legs of flight intercomparisons between 0.2 and 5.3 km (Eisele et al., 2003), although this bias from TRACE-P intercomparisons is resolved by the revision of the ATHOS calibration factor for measurements from 2001 to 2006 (Ren et al., 2008). A more recent aircraft intercomparison was conducted during the NASA ARTCAS aircraft campaign, in which the same two instruments were both installed on NASA DC-8 aircraft and therefore provides a far more detailed examination. During ARCTAS, the campaign-average ratio of LIF/CIMS OH is roughly 1.03, suggesting a good agreement for the two instruments in a clean atmosphere (Ren et al., 2012).

Ground comparisons for OH measurements were conducted in both ambient air and chamber tests. For chamber tests and clean air in rural sites, good agreement was achieved between LIF instruments and DOAS instruments, including POPCORN

Insights into hydroxyl measurements in a forest

J. Mao et al.

Title Page

Abstract

Introduction

Conclusions

References

Tables

Figures



Back

Close

Full Screen / Esc

Printer-friendly Version

Interactive Discussion



field campaign (Brauers et al., 1996), and SAPHIR chamber tests (Schlosser et al., 2007, 2009). In addition, these intercomparisons rule out the possible interference from ozone photolysis inside the LIF instruments, consistent with our tests. For a forest atmosphere, however, a persistent discrepancy was revealed between CIMS instrument and three LIF instruments, in which CIMS measured OH is unilaterally less than all other LIF measured OH by 30–40 % (Table 4 in Schlosser et al., 2009), further supporting our conclusion in this study. In fact, isoprene concentrations mainly ranged between 0.3 and 0.6 ppb during the intercomparison period for that study (Schlosser et al., 2009), far less than the biogenic VOC level encountered in BEARPEX09 (Table S1). Therefore we expect this discrepancy between OHwave and OHchem to be larger during BEARPEX09.

The conclusion that the measurement of OH by chemical modulation, OHchem, is the real atmospheric OH is supported by indirect evidence from the BEARPEX07 study (<http://www.ocf.berkeley.edu/~bearpex/>), including the greatly improved agreement for acyl peroxy nitrates (LaFranchi et al., 2009) and glyoxal (Huisman et al., 2011) when the model is constrained with a scaled OHwave using the measured OHchem to OHwave ratios during BEARPEX09. Thus, these measurements of OH, HO₂, and OH reactivity are generally consistent with our understanding of BVOC oxidation chemistry as represented in the model with recent updates in BVOC oxidation mechanisms.

Laboratory studies are underway to identify the source of the difference between OHwave and OHchem and to quantify the amount of the interference that may be removed by the external addition of C₃F₆. However, identifying the cause of the OH interference and determining its possible relevance to atmospheric processes will take some time. So it will be difficult to reduce the uncertainty in the “real OH” measured by the Penn State LIF instrument until the identity of the OH interference is complete. On the other hand, it is important for the chemistry modeling community to know that measurements of unexpectedly large OH may not be correct for all forested environments and that they should wait before implementing this chemistry in their models until the measurement issues are resolved.

Insights into hydroxyl measurements in a forest

J. Mao et al.

[Title Page](#)[Abstract](#)[Introduction](#)[Conclusions](#)[References](#)[Tables](#)[Figures](#)[⏪](#)[⏩](#)[◀](#)[▶](#)[Back](#)[Close](#)[Full Screen / Esc](#)[Printer-friendly Version](#)[Interactive Discussion](#)

Caution must be taken for applying this discrepancy to other LIF instruments. Instrument designs differ significantly among LIF instruments in terms of flow geometry, pumping speed, cell pressure, laser frequency and optical paths in the detection cell. These differences can certainly cause difference in supersonic expansion, temperature profile from inlet to the detection region, and flow residence time, which will lead to difference in the amount of internally produced OH. This question could be answered by deploying the second method of OH measurement on other LIF instruments.

This difference may also vary among different forested environments. If the difference between OH_{wave} and OH_{chem} is solely driven by ozone chemistry (ozonolysis of BVOCs), such difference would then be sensitive to ambient ozone concentrations. In particular, in contrast to a mean of 54 ppb ozone in BEARPEX09, observed daytime ozone in tropical forests can be as low as 10 to 20 ppb (Lelieveld et al., 2008; Stone et al., 2011). On the other hand, if such discrepancy is partly contributed by OH-driven chemistry (for example by HPALDs), the discrepancy may be less dependent of ozone concentrations. Further investigation is needed on these hypotheses.

This consistency between measured OH, HO₂, and OH reactivity applies only to the Sierra Nevada forest in the BEARPEX09 study. It is not clear whether these findings also apply to other forest atmospheres or to the OH measurements with other FAGE-type instruments in other forests. Only measurements in those forest atmospheres with other FAGE-type instruments will resolve this question.

Supplementary material related to this article is available online at:
[http://www.atmos-chem-phys-discuss.net/12/6715/2012/
acpd-12-6715-2012-supplement.pdf](http://www.atmos-chem-phys-discuss.net/12/6715/2012/acpd-12-6715-2012-supplement.pdf).

Acknowledgements. We acknowledge the contributions from Jennifer Gielen and Josh Magerman for HO_x measurements and from Robin Weber for CO and O₃ measurements during BEARPEX09 study. We acknowledge the contributions from Li Zhang for laboratory experiments in quantifying the internal generated OH. We also acknowledge William Stockwell and Wendy Goliff for the RACM2 mechanism. We thank Sierra Pacific Industries for the use of their

Insights into hydroxyl measurements in a forest

J. Mao et al.

Title Page

Abstract

Introduction

Conclusions

References

Tables

Figures

◀

▶

◀

▶

Back

Close

Full Screen / Esc

Printer-friendly Version

Interactive Discussion



land and the University of California, Berkeley, Center for Forestry, Blodgett Forest Research Station for cooperation in facilitating this research. AHG would like to acknowledge NSF Atmospheric Chemistry Program Grant # 0922562. FNK would like to acknowledge NSF Atmospheric Chemistry Program Grant # 0852406.

5 References

Baasandorj, M. and Stevens, P. S.: Experimental and theoretical studies of the kinetics of the reactions of OH and OD with 2-methyl-3-buten-2-ol between 300 and 415 K at low pressure, *J. Phys. Chem. A*, 111, 640–649, doi:10.1021/jp066286x, 2007.

10 Bouvier-Brown, N. C., Goldstein, A. H., Gilman, J. B., Kuster, W. C., and de Gouw, J. A.: In-situ ambient quantification of monoterpenes, sesquiterpenes, and related oxygenated compounds during BEARPEX 2007: implications for gas- and particle-phase chemistry, *Atmos. Chem. Phys.*, 9, 5505–5518, doi:10.5194/acp-9-5505-2009, 2009a.

15 Bouvier-Brown, N. C., Goldstein, A. H., Worton, D. R., Matross, D. M., Gilman, J. B., Kuster, W. C., Welsh-Bon, D., Warneke, C., de Gouw, J. A., Cahill, T. M., and Holzinger, R.: Methyl chavicol: characterization of its biogenic emission rate, abundance, and oxidation products in the atmosphere, *Atmos. Chem. Phys.*, 9, 2061–2074, doi:10.5194/acp-9-2061-2009, 2009b.

20 Bouvier-Brown, N. C., Holzinger, R., Palitzsch, K., and Goldstein, A. H.: Large emissions of sesquiterpenes and methyl chavicol quantified from branch enclosure measurements, *Atmos. Environ.*, 43, 389–401, doi:10.1016/j.atmosenv.2008.08.039, 2009c.

Brauers, T., Aschmutat, U., Brandenburger, U., Dorn, H. P., Hausmann, M., Heßling, M., Hofzumahaus, A., Holland, F., Plass-Dülmer, C., and Ehhalt, D. H.: Intercomparison of tropospheric OH radical measurements by multiple folded long path laser absorption and laser induced fluorescence, *Geophys. Res. Lett.*, 23, 2545–2548, doi:10.1029/96gl02204, 1996.

25 Butler, T. M., Taraborrelli, D., Brühl, C., Fischer, H., Harder, H., Martinez, M., Williams, J., Lawrence, M. G., and Lelieveld, J.: Improved simulation of isoprene oxidation chemistry with the ECHAM5/MESSy chemistry-climate model: lessons from the GABRIEL airborne field campaign, *Atmos. Chem. Phys.*, 8, 4529–4546, doi:10.5194/acp-8-4529-2008, 2008.

30 Carrasco, N., Doussin, J. F., O'Connor, M., Wenger, J. C., Picquet-Varrault, B., Durand-Jolibois, R., and Carlier, P.: Simulation chamber studies of the atmospheric oxidation of

ACPD

12, 6715–6744, 2012

Insights into hydroxyl measurements in a forest

J. Mao et al.

Title Page

Abstract

Introduction

Conclusions

References

Tables

Figures

◀

▶

◀

▶

Back

Close

Full Screen / Esc

Printer-friendly Version

Interactive Discussion



Insights into hydroxyl measurements in a forest

J. Mao et al.

[Title Page](#)[Abstract](#)[Introduction](#)[Conclusions](#)[References](#)[Tables](#)[Figures](#)[◀](#)[▶](#)[◀](#)[▶](#)[Back](#)[Close](#)[Full Screen / Esc](#)[Printer-friendly Version](#)[Interactive Discussion](#)

2-methyl-3-buten-2-ol: reaction with hydroxyl radicals and ozone under a variety of conditions, *J. Atmos. Chem.*, 56, 33–55, doi:10.1007/s10874-006-9041-y, 2007.

Chan, A. W. H., Galloway, M. M., Kwan, A. J., Chhabra, P. S., Keutsch, F. N., Wennberg, P. O., Flagan, R. C., and Seinfeld, J. H.: Photooxidation of 2-Methyl-3-Buten-2-ol (MBO) as a potential source of secondary organic aerosol, *Environ. Sci. Technol.*, 43, 4647–4652, doi:10.1021/es802560w, 2009.

Crounse, J. D., Paulot, F., Kjaergaard, H. G., and Wennberg, P. O.: Peroxy radical isomerization in the oxidation of isoprene, *Phys. Chem. Chem. Phys.*, 13, 13607–13613, doi:10.1039/C1CP21330J 2011.

Di Carlo, P., Brune, W. H., Martinez, M., Harder, H., Leshner, R., Ren, X. R., Thornberry, T., Carroll, M. A., Young, V., Shepson, P. B., Riemer, D., Apel, E., and Campbell, C.: Missing OH reactivity in a forest: evidence for unknown reactive biogenic VOCs, *Science*, 304, 722–725, 2004.

Donahue, N. M., Drozd, G. T., Epstein, S. A., Presto, A. A., and Kroll, J. H.: Adventures in ozoneland: down the rabbit-hole, *Phys. Chem. Chem. Phys.*, 13, 10848–10857, 2011.

Dreyfus, G. B., Schade, G. W., and Goldstein, A. H.: Observational constraints on the contribution of isoprene oxidation to ozone production on the western slope of the Sierra Nevada, California, *J. Geophys. Res.-Atmos.*, 107, 4365 pp., doi:10.1029/2001jd001490, 2002.

Dubey, M. K., Hanisco, T. F., Wennberg, P. O., and Anderson, J. G.: Monitoring potential photochemical interference in laser-induced fluorescence measurements of atmospheric OH, *Geophys. Res. Lett.*, 23, 3215–3218, 1996.

Eisele, F. L., Mauldin, R. L., Tanner, D. J., Cantrell, C., Kosciuch, E., Nowak, J. B., Brune, B., Faloon, I., Tan, D., Davis, D. D., Wang, L., and Chen, G.: Relationship between OH measurements on two different NASA aircraft during PEM Tropics B, *J. Geophys. Res.-Atmos.*, 106, 32683–32689, 2001.

Eisele, F. L., Mauldin, L., Cantrell, C., Zondlo, M., Apel, E., Fried, A., Walega, J., Shetter, R., Lefer, B., Flocke, F., Weinheimer, A., Avery, M., Vay, S., Sachse, G., Podolske, J., Diskin, G., Barrick, J. D., Singh, H. B., Brune, W., Harder, H., Martinez, M., Bandy, A., Thornton, D., Heikes, B., Kondo, Y., Riemer, D., Sandholm, S., Tan, D., Talbot, R., and Dibb, J.: Summary of measurement intercomparisons during TRACE-P, *J. Geophys. Res.*, 108, 8791, doi:10.1029/2002jd003167, 2003.

Faloon, I., Tan, D., Brune, W., Hurst, J., Barkot, D., Couch, T. L., Shepson, P., Apel, E., Riemer, D., Thornberry, T., Carroll, M. A., Sillman, S., Keeler, G. J., Sagady, J., Hooper, D.,

Insights into hydroxyl measurements in a forest

J. Mao et al.

Title Page

Abstract

Introduction

Conclusions

References

Tables

Figures

◀

▶

◀

▶

Back

Close

Full Screen / Esc

Printer-friendly Version

Interactive Discussion



and Paterson, K.: Nighttime observations of anomalously high levels of hydroxyl radicals above a deciduous forest canopy, *J. Geophys. Res.-Atmos.*, 106, 24315–24333, 2001.

Faloon, I. C., Tan, D., Leshner, R. L., Hazen, N. L., Frame, C. L., Simpas, J. B., Harder, H., Martinez, M., Di Carlo, P., Ren, X. R., and Brune, W. H.: A laser-induced fluorescence instrument for detecting tropospheric OH and HO₂: characteristics and calibration, *J. Atmos. Chem.*, 47, 139–167, 2004.

Fares, S., McKay, M., Holzinger, R., and Goldstein, A. H.: Ozone fluxes in a *Pinus ponderosa* ecosystem are dominated by non-stomatal processes: evidence from long-term continuous measurements, *Agr. Forest Meteorol.*, 150, 420–431, doi:10.1016/j.agrformet.2010.01.007, 2010.

Fuchs, H., Bohn, B., Hofzumahaus, A., Holland, F., Lu, K. D., Nehr, S., Rohrer, F., and Wahner, A.: Detection of HO₂ by laser-induced fluorescence: calibration and interferences from RO₂ radicals, *Atmos. Meas. Tech.*, 4, 1209–1225, doi:10.5194/amt-4-1209-2011, 2011.

Hansen, M. C., DeFries, R. S., Townshend, J. R. G., Carroll, M., Dimiceli, C., and Sohlberg, R. A.: Global percent tree cover at a spatial resolution of 500 m: first results of the MODIS vegetation continuous fields algorithm, *Earth Interact.*, 7, 10, 2003.

Hard, T. M., O'Brien, R. J., Chan, C. Y., and Mehrabzadeh, A. A.: Tropospheric free radical determination by fluorescence assay with gas expansion, *Environ. Sci. Technol.*, 18, 768–777, doi:10.1021/es00128a009, 1984.

Heal, M. R., Heard, D. E., Pilling, M. J., and Whitaker, B. J.: On the development and validation of FAGE for local measurement of tropospheric OH and HO₂, *J. Atmos. Sci.*, 52, 3428–3441, doi:10.1175/1520-0469(1995)052<3428:otdavo>2.0.co;2, 1995.

Henderson, B. H., Pinder, R. W., Crooks, J., Cohen, R. C., Hutzell, W. T., Sarwar, G., Gollif, W. S., Stockwell, W. R., Fahr, A., Mathur, R., Carlton, A. G., and Vizuete, W.: Evaluation of simulated photochemical partitioning of oxidized nitrogen in the upper troposphere, *Atmos. Chem. Phys.*, 11, 275–291, doi:10.5194/acp-11-275-2011, 2011.

Herrmann, F., Winterhalter, R., Moortgat, G. K., and Williams, J.: Hydroxyl radical (OH) yields from the ozonolysis of both double bonds for five monoterpenes, *Atmos. Environ.*, 44, 3458–3464, doi:10.1016/j.atmosenv.2010.05.011, 2010.

Hofzumahaus, A., Rohrer, F., Lu, K. D., Bohn, B., Brauers, T., Chang, C. C., Fuchs, H., Holland, F., Kita, K., Kondo, Y., Li, X., Lou, S. R., Shao, M., Zeng, L. M., Wahner, A., and Zhang, Y. H.: Amplified trace gas removal in the troposphere, *Science*, 324, 1702–1704, doi:10.1126/science.1164566, 2009.

Insights into hydroxyl measurements in a forest

J. Mao et al.

Title Page

Abstract

Introduction

Conclusions

References

Tables

Figures

◀

▶

◀

▶

Back

Close

Full Screen / Esc

Printer-friendly Version

Interactive Discussion



Holzinger, R., Lee, A., Paw, K. T., and Goldstein, U. A. H.: Observations of oxidation products above a forest imply biogenic emissions of very reactive compounds, *Atmos. Chem. Phys.*, 5, 67–75, doi:10.5194/acp-5-67-2005, 2005.

Huisman, A. J., Hottle, J. R., Galloway, M. M., DiGangi, J. P., Coens, K. L., Choi, W., Faloon, I. C., Gilman, J. B., Kuster, W. C., de Gouw, J., Bouvier-Brown, N. C., Goldstein, A. H., LaFranchi, B. W., Cohen, R. C., Wolfe, G. M., Thornton, J. A., Docherty, K. S., Farmer, D. K., Cubison, M. J., Jimenez, J. L., Mao, J., Brune, W. H., and Keutsch, F. N.: Photochemical modeling of glyoxal at a rural site: observations and analysis from BEARPEX 2007, *Atmos. Chem. Phys.*, 11, 8883–8897, doi:10.5194/acp-11-8883-2011, 2011.

Kanaya, Y., Hofzumahaus, A., Dorn, H.-P., Brauers, T., Fuchs, H., Holland, F., Rohrer, F., Bohn, B., Tillmann, R., Wegener, R., Wahner, A., Kajii, Y., Miyamoto, K., Nishida, S., Watanabe, K., Yoshino, A., Kubistin, D., Martinez, M., Rudolf, M., Harder, H., Berresheim, H., Elste, T., Plass-Dülmer, C., Stange, G., Kleffmann, J., Elshorbany, Y., and Schurath, U.: Comparisons of observed and modeled OH and HO₂ concentrations during the ambient measurement period of the HO_xComp field campaign, *Atmos. Chem. Phys. Discuss.*, 11, 28851–28894, doi:10.5194/acpd-11-28851-2011, 2011.

Karl, T., Harley, P., Emmons, L., Thornton, B., Guenther, A., Basu, C., Turnipseed, A., and Jardine, K.: Efficient atmospheric cleansing of oxidized organic trace gases by vegetation, *Science*, 330, 816–819, doi:10.1126/science.1192534, 2010.

Kim, S., Guenther, A., Karl, T., and Greenberg, J.: Contributions of primary and secondary biogenic VOC to total OH reactivity during the CABINEX (Community Atmosphere-Biosphere Interactions Experiments)-09 field campaign, *Atmos. Chem. Phys.*, 11, 8613–8623, doi:10.5194/acp-11-8613-2011, 2011.

Kroll, J. H., Sahay, S. R., Anderson, J. G., Demerjian, K. L., and Donahue, N. M.: Mechanism of HO_x formation in the gas-phase ozone-alkene reaction. 2. Prompt versus thermal dissociation of carbonyl oxides to form OH, *J. Phys. Chem. A*, 105, 4446–4457, doi:10.1021/jp004136v, 2001.

Kurpius, M. R. and Goldstein, A. H.: Gas-phase chemistry dominates O₃ loss to a forest, implying a source of aerosols and hydroxyl radicals to the atmosphere, *Geophys. Res. Lett.*, 30, 1371, doi:10.1029/2002gl016785, 2003.

LaFranchi, B. W., Wolfe, G. M., Thornton, J. A., Harrold, S. A., Browne, E. C., Min, K. E., Wooldridge, P. J., Gilman, J. B., Kuster, W. C., Goldan, P. D., de Gouw, J. A., McKay, M., Goldstein, A. H., Ren, X., Mao, J., and Cohen, R. C.: Closing the peroxy acetyl nitrate budget:

Insights into hydroxyl measurements in a forest

J. Mao et al.

[Title Page](#)[Abstract](#)[Introduction](#)[Conclusions](#)[References](#)[Tables](#)[Figures](#)[◀](#)[▶](#)[◀](#)[▶](#)[Back](#)[Close](#)[Full Screen / Esc](#)[Printer-friendly Version](#)[Interactive Discussion](#)

observations of acyl peroxy nitrates (PAN, PPN, and MPAN) during BEARPEX 2007, *Atmos. Chem. Phys.*, 9, 7623–7641, doi:10.5194/acp-9-7623-2009, 2009.

Lelieveld, J., Butler, T. M., Crowley, J. N., Dillon, T. J., Fischer, H., Ganzeveld, L., Harder, H., Lawrence, M. G., Martinez, M., Taraborrelli, D., and Williams, J.: Atmospheric oxidation capacity sustained by a tropical forest, *Nature*, 452, 737–740, doi:10.1038/nature06870, 2008.

Lou, S., Holland, F., Rohrer, F., Lu, K., Bohn, B., Brauers, T., Chang, C.C., Fuchs, H., Häsel, R., Kita, K., Kondo, Y., Li, X., Shao, M., Zeng, L., Wahner, A., Zhang, Y., Wang, W., and Hofzumahaus, A.: Atmospheric OH reactivities in the Pearl River Delta – China in summer 2006: measurement and model results, *Atmos. Chem. Phys.*, 10, 11243–11260, doi:10.5194/acp-10-11243-2010, 2010.

Lu, K. D., Rohrer, F., Holland, F., Fuchs, H., Bohn, B., Brauers, T., Chang, C. C., Häsel, R., Hu, M., Kita, K., Kondo, Y., Li, X., Lou, S. R., Nehr, S., Shao, M., Zeng, L. M., Wahner, A., Zhang, Y. H., and Hofzumahaus, A.: Observation and modelling of OH and HO₂ concentrations in the Pearl River Delta 2006: a missing OH source in a VOC rich atmosphere, *Atmos. Chem. Phys.*, 12, 1541–1569, doi:10.5194/acp-12-1541-2012, 2012.

Mao, J., Ren, X., Brune, W. H., Olson, J. R., Crawford, J. H., Fried, A., Huey, L. G., Cohen, R. C., Heikes, B., Singh, H. B., Blake, D. R., Sachse, G. W., Diskin, G. S., Hall, S. R., and Shetter, R. E.: Airborne measurement of OH reactivity during INTEX-B, *Atmos. Chem. Phys.*, 9, 163–173, doi:10.5194/acp-9-163-2009, 2009.

Paulot, F., Crounse, J. D., Kjaergaard, H. G., Kroll, J. H., Seinfeld, J. H., and Wennberg, P. O.: Isoprene photooxidation: new insights into the production of acids and organic nitrates, *Atmos. Chem. Phys.*, 9, 1479–1501, doi:10.5194/acp-9-1479-2009, 2009a.

Paulot, F., Crounse, J. D., Kjaergaard, H. G., Kurten, A., St Clair, J. M., Seinfeld, J. H., and Wennberg, P. O.: Unexpected epoxide formation in the gas-phase photooxidation of isoprene, *Science*, 325, 730–733, doi:10.1126/science.1172910, 2009b.

Peeters, J. and Müller, J. F.: HO_x radical regeneration in isoprene oxidation via peroxy radical isomerisations. II: experimental evidence and global impact, *Phys. Chem. Chem. Phys.*, 12, 14227–14235, doi:10.1039/c0cp00811g, 2010.

Peeters, J., Nguyen, T. L., and Vereecken, L.: HO_x radical regeneration in the oxidation of isoprene, *Phys. Chem. Chem. Phys.*, 11, 5935–5939, doi:10.1039/b908511d, 2009.

Ren, X. R., Harder, H., Martinez, M., Faloon, I. C., Tan, D., Leshner, R. L., Di Carlo, P., Simpas, J. B., and Brune, W. H.: Interference testing for atmospheric HO_x measurements by

Insights into hydroxyl measurements in a forest

J. Mao et al.

Title Page

Abstract

Introduction

Conclusions

References

Tables

Figures

◀

▶

◀

▶

Back

Close

Full Screen / Esc

Printer-friendly Version

Interactive Discussion



laser-induced fluorescence, *J. Atmos. Chem.*, 47, 169–190, 2004.

Ren, X. R., Olson, J. R., Crawford, J. H., Brune, W. H., Mao, J. Q., Long, R. B., Chen, Z., Chen, G., Avery, M. A., Sachse, G. W., Barrick, J. D., Diskin, G. S., Huey, L. G., Fried, A., Cohen, R. C., Heikes, B., Wennberg, P. O., Singh, H. B., Blake, D. R., and Shetter, R. E.: HO_x chemistry during INTEX-A 2004: observation, model calculation, and comparison with previous studies, *J. Geophys. Res.-Atmos.*, 113(13), D05310, doi:10.1029/2007jd009166, 2008.

Schade, G. W., Goldstein, A. H., Gray, D. W., and Lerdau, M. T.: Canopy and leaf level 2-methyl-3-buten-2-ol fluxes from a ponderosa pine plantation, *Atmos. Environ.*, 34, 3535–3544, 2000.

Schlosser, E., Bohn, B., Brauers, T., Dorn, H.-P., Fuchs, H., Häsel, R., Hofzumahaus, A., Holland, F., Rohrer, F., Rupp, L., Siese, M., Tillmann, R., and Wahner, A.: Intercomparison of two hydroxyl radical measurement techniques at the atmosphere simulation chamber SAPHIR, *J. Atmos. Chem.*, 56, 187–205, doi:10.1007/s10874-006-9049-3, 2007.

Schlosser, E., Brauers, T., Dorn, H.-P., Fuchs, H., Häsel, R., Hofzumahaus, A., Holland, F., Wahner, A., Kanaya, Y., Kajii, Y., Miyamoto, K., Nishida, S., Watanabe, K., Yoshino, A., Kubistin, D., Martinez, M., Rudolf, M., Harder, H., Berresheim, H., Elste, T., Plass-Dülmer, C., Stange, G., and Schurath, U.: Technical Note: Formal blind intercomparison of OH measurements: results from the international campaign HOxComp, *Atmos. Chem. Phys.*, 9, 7923–7948, doi:10.5194/acp-9-7923-2009, 2009.

Smith, G. P. and Crosley, D. R.: A photochemical model of ozone interference effects in laser detection of tropospheric OH, *J. Geophys. Res.*, 95, 16427–16442, doi:10.1029/JD095iD10p16427, 1990.

Steiner, A. L., Tonse, S., Cohen, R. C., Goldstein, A. H., and Harley, R. A.: Biogenic 2-methyl-3-buten-2-ol increases regional ozone and HO_x sources, *Geophys. Res. Lett.*, 34, L15806, doi:10.1029/2007gl030802, 2007.

Stevens, P. S., Mather, J. H., and Brune, W. H.: Measurement of tropospheric OH and HO₂ by laser-induced fluorescence at low pressure, *J. Geophys. Res.*, 99, 3543–3557, doi:10.1029/93jd03342, 1994.

Stone, D., Evans, M. J., Edwards, P. M., Commane, R., Ingham, T., Rickard, A. R., Brookes, D. M., Hopkins, J., Leigh, R. J., Lewis, A. C., Monks, P. S., Oram, D., Reeves, C. E., Stewart, D., and Heard, D. E.: Isoprene oxidation mechanisms: measurements and modelling of OH and HO₂ over a South-East Asian tropical rainforest during the OP3 field

Insights into hydroxyl measurements in a forest

J. Mao et al.

[Title Page](#)[Abstract](#)[Introduction](#)[Conclusions](#)[References](#)[Tables](#)[Figures](#)[◀](#)[▶](#)[◀](#)[▶](#)[Back](#)[Close](#)[Full Screen / Esc](#)[Printer-friendly Version](#)[Interactive Discussion](#)

campaign, *Atmos. Chem. Phys.*, 11, 6749–6771, doi:10.5194/acp-11-6749-2011, 2011.

Tan, D., Faloon, I., Simpas, J. B., Brune, W., Shepson, P. B., Couch, T. L., Sumner, A. L., Carroll, M. A., Thornberry, T., Apel, E., Riemer, D., and Stockwell, W.: HO_x budgets in a deciduous forest: results from the PROPHET summer 1998 campaign, *J. Geophys. Res.-Atmos.*, 106, 24407–24427, 2001.

Tanner, D. J., Jefferson, A., and Eisele, F. L.: Selected ion chemical ionization mass spectrometric measurement of OH, *J. Geophys. Res.*, 102, 6415–6425, doi:10.1029/96jd03919, 1997.

Thornton, J. A., Wooldridge, P. J., Cohen, R. C., Martinez, M., Harder, H., Brune, W. H., Williams, E. J., Roberts, J. M., Fehsenfeld, F. C., Hall, S. R., Shetter, R. E., Wert, B. P., and Fried, A.: Ozone production rates as a function of NO_x abundances and HO_x production rates in the Nashville urban plume, *J. Geophys. Res.*, 107, 4146, doi:10.1029/2001jd000932, 2002.

Whalley, L. K., Edwards, P. M., Furneaux, K. L., Goddard, A., Ingham, T., Evans, M. J., Stone, D., Hopkins, J. R., Jones, C. E., Karunaharan, A., Lee, J. D., Lewis, A. C., Monks, P. S., Moller, S. J., and Heard, D. E.: Quantifying the magnitude of a missing hydroxyl radical source in a tropical rainforest, *Atmos. Chem. Phys.*, 11, 7223–7233, doi:10.5194/acp-11-7223-2011, 2011.

Wolfe, G. M. and Thornton, J. A.: The Chemistry of Atmosphere-Forest Exchange (CAFE) Model – Part 1: Model description and characterization, *Atmos. Chem. Phys.*, 11, 77–101, doi:10.5194/acp-11-77-2011, 2011.

Wolfe, G. M., Thornton, J. A., Bouvier-Brown, N. C., Goldstein, A. H., Park, J.-H., McKay, M., Matross, D. M., Mao, J., Brune, W. H., LaFranchi, B. W., Browne, E. C., Min, K.-E., Wooldridge, P. J., Cohen, R. C., Crouse, J. D., Faloon, I. C., Gilman, J. B., Kuster, W. C., de Gouw, J. A., Huisman, A., and Keutsch, F. N.: The Chemistry of Atmosphere-Forest Exchange (CAFE) Model – Part 2: Application to BEARPEX-2007 observations, *Atmos. Chem. Phys.*, 11, 1269–1294, doi:10.5194/acp-11-1269-2011, 2011.

Zhang, D., Lei, W. F., and Zhang, R. Y.: Mechanism of OH formation from ozonolysis of isoprene: kinetics and product yields, *Chem. Phys. Lett.*, 358, 171–179, 2002.

Insights into hydroxyl measurements in a forest

J. Mao et al.

Title Page

Abstract

Introduction

Conclusions

References

Tables

Figures

◀

▶

◀

▶

Back

Close

Full Screen / Esc

Printer-friendly Version

Interactive Discussion



Table 1. VOCs and other chemical species measured and used in the OH reactivity calculation. Also listed are the unmeasured but modeled species that could be major contributors to OH reactivity.

Measured species		
α -Pinene	HCHO	Acetonitrile
β -Pinene	Acetaldehyde	HNO ₃
Isoprene	Isoprene hydroxyhydroperoxide	MPAN
Methylbutenol (MBO)	Glyoxal	PAN
Methyl vinyl ketone (MVK)	Glycolaldehyde	PPN
Methacrolein (MACR)	Hydroxyacetone	NO ₂
Unidentified sesquiterpenes	Methanol	CO
Methyl Chavicol	Ethanol	HONO
Camphene	Butanol	NO
Acetone	Isobutyl alcohol	O ₃
Benzene	Toluene	Butane
Unmeasured species as major contributors to OH reactivity		
MBO oxidation products (2.2) *		
Isoprene epoxides (0.9)		
C3 and higher aldehydes (1.6)		

*: The numbers in the brackets indicate the median OH loss rates at 303 K in the model with the units of s⁻¹.

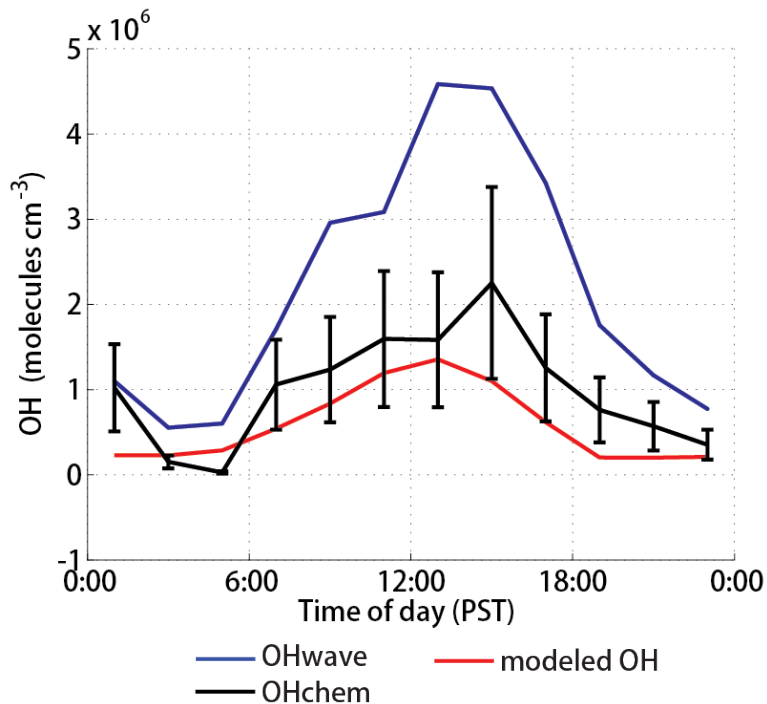


Fig. 1. Diurnal cycle of measured and modeled OH between 20 June and 30 July 2009 near the Blodgett Forest Research Station (BFRS). “OHwave” (blue line) is statistically different from “OHchem” (black line) and modeled OH (red line). The model incorporates the current understanding of BVOC oxidation chemistry (see text for details). The vertical bars indicate OHchem’s absolute uncertainty of $\pm 50\%$ (2σ confidence), which comes from combining the uncertainty from the internally generated OH removed by the C_3F_6 addition used to measure OHchem ($\pm 30\%$) and the absolute uncertainty of the OH measurements ($\pm 40\%$ at 2σ confidence). OHchem, which is shown to be equal to or greater than the real OH, is similar to modeled OH, indicating a generally good understanding of oxidation in this forest atmosphere.

Insights into hydroxyl measurements in a forest

J. Mao et al.

Title Page	
Abstract	Introduction
Conclusions	References
Tables	Figures
◀	▶
◀	▶
Back	Close
Full Screen / Esc	
Printer-friendly Version	
Interactive Discussion	



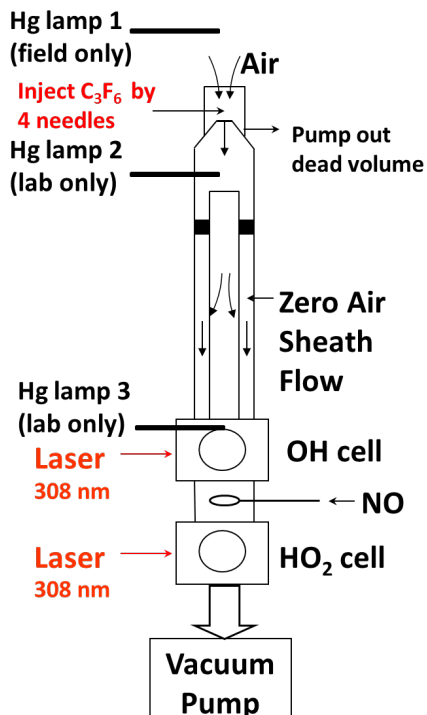


Fig. 2. Schematic diagram of the detection system cross section. Gaseous C_3F_6 was injected simultaneously through four 0.25 mm needles pointed toward the center, which were located about 4 cm above the inlet. Hg lamp 1 was deployed in the field only to ensure that the C_3F_6 or propane removed most of the externally generated OH. Hg lamp 2 and 3 were installed in the lab only to determine how much OH is removed internally with the external C_3F_6 addition. Hg lamp 2 was added just under the inlet cone. Hg lamp 3 was inserted in the ring just above the OH detection cell and shone light into the sheath flow and the detection axis. Both lamp 2 and 3 were shrouded so that the light just went across the flow tube directly and not down or up.

Insights into hydroxyl measurements in a forest

J. Mao et al.

Title Page

Abstract Introduction

Conclusions References

Tables Figures

◀ ▶

◀ ▶

Back Close

Full Screen / Esc

Printer-friendly Version

Interactive Discussion



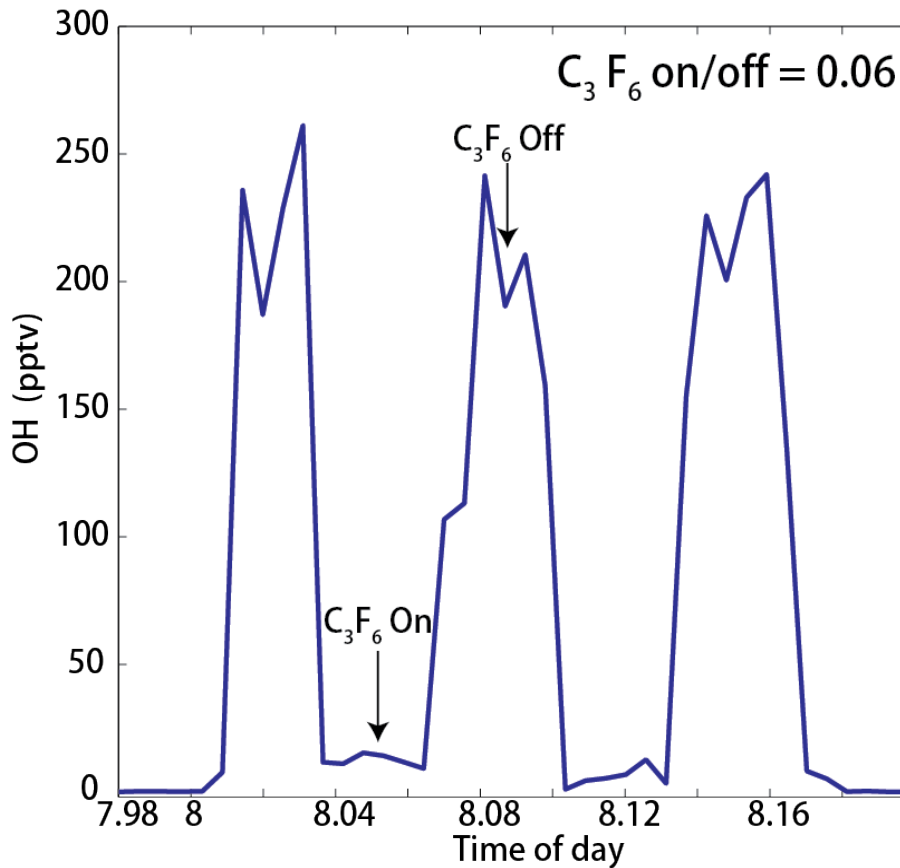


Fig. 3. Example of OH measurement with an external mercury lamp (Hg lamp 1 in Fig. 1) producing OH and periodic C_3F_6 addition. The large OH value is when C_3F_6 is not added and the small value occurs when it is. The removal efficiency for this example is 94 %.

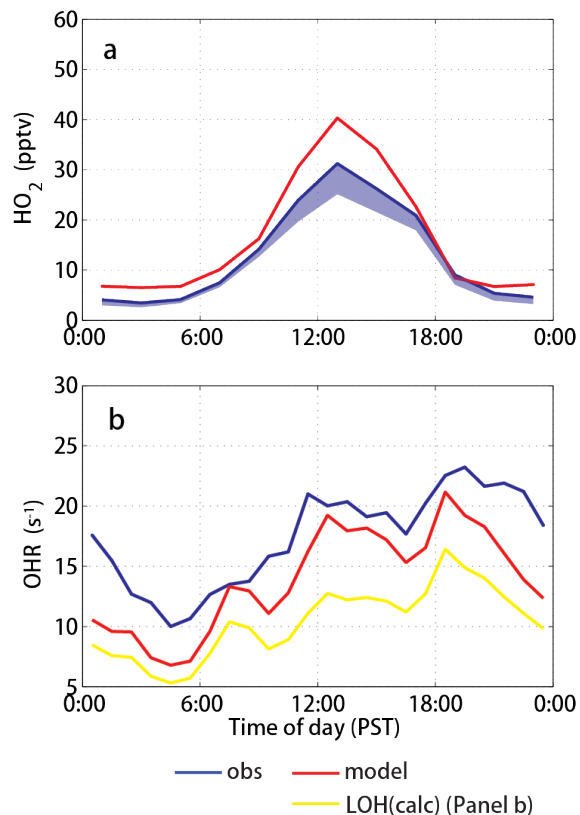


Fig. 4. Diurnal cycle of HO₂ (a) and OH reactivity (b) between 20 June and 30 July 2009 near the Blodgett Forest Research Station (BFRS). In the top panel, the shaded area below measured HO₂ (blue open circles) indicates the contribution to measured HO₂ from an RO₂ interference from isoprene, MVK and MACR (Fuchs et al., 2011). In the bottom panel, the calculated OH reactivity from available measurements (LOH) is represented by a yellow line. The absolute uncertainty of the HO₂ measurements is $\pm 40\%$ at 2σ confidence. The absolute uncertainty of OH reactivity measurement is 1 s^{-1} at 2σ confidence (Mao et al., 2009). The model incorporates the current understanding of BVOC oxidation chemistry (see text for details).

Insights into hydroxyl measurements in a forest

J. Mao et al.

Title Page

Abstract Introduction

Conclusions References

Tables Figures

◀ ▶

◀ ▶

Back Close

Full Screen / Esc

Printer-friendly Version

Interactive Discussion



Insights into hydroxyl measurements in a forest

J. Mao et al.

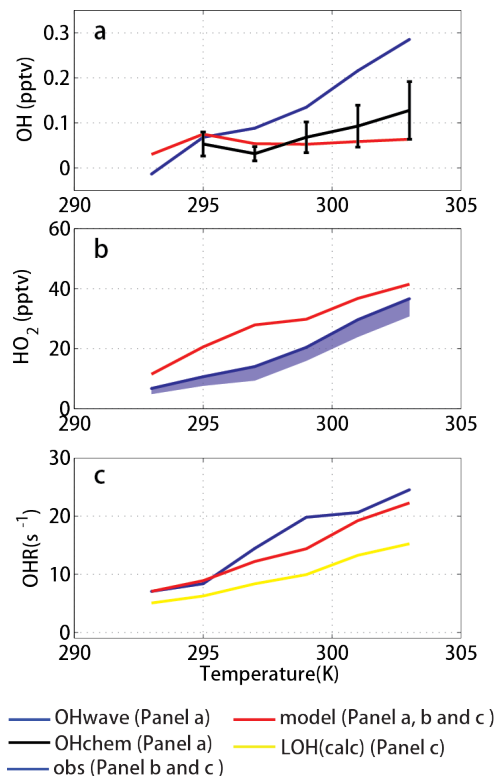


Fig. 5. Temperature dependence of (a) daytime measured and modeled OH, (b) daytime measured and modeled HO₂, and (c) OH reactivity between 09:00 and 15:00 PST during BEARPEX09. In panel (a), “OHwave” (blue line) grows significantly greater than “OHchem” (black line) and modeled OH (red line), which show little temperature dependence. The vertical bars indicate a combined uncertainty as described in Fig. 1. In panel (b), measured HO₂ (blue line) is lower than modeled HO₂ (red line) but not significantly at the low and high temperatures. Measured HO₂ may be affected by an RO₂ interference from isoprene, MVK and MACR (Fuchs et al., 2011), as indicated by the blue shading. In panel (c), the difference between the measured OH reactivity (blue line) and the OH reactivity calculated from available measurements (yellow line) suggests missing OH reactivity, which is mostly resolved when including modeled intermediates (red line) in the calculation.

Title Page

Abstract

Introduction

Conclusions

References

Tables

Figures

◀

▶

◀

▶

Back

Close

Full Screen / Esc

Printer-friendly Version

Interactive Discussion



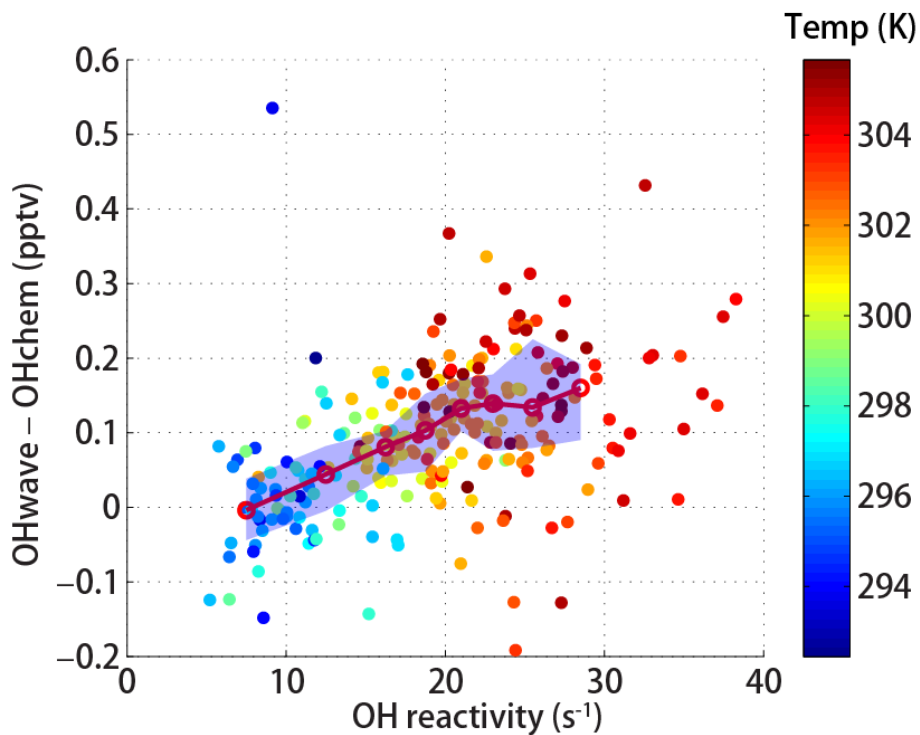


Fig. 6. Scatter plot between the measured OH reactivity and the difference between OHchem and OHwave between 09:00 and 15:00 PST. The 10-min averaged points are colored by the ambient temperature. The shaded blue area is the interquartile range of the data and the open circles are the median values in temperature bins.

Insights into hydroxyl measurements in a forest

J. Mao et al.

Title Page

Abstract Introduction

Conclusions References

Tables Figures

◀ ▶

◀ ▶

Back Close

Full Screen / Esc

Printer-friendly Version

Interactive Discussion

